February 2012

Particle transport over rough hillslope surfaces by dry ravel: Experiments and simulations with implications for nonlocal sediment flux

Emmanuel Gabet
San Jose State University, manny.gabet@sjsu.edu

Morgan Mendoza
San Jose State University

Recommended Citation

Emmanuel Gabet and Morgan Mendoza. "Particle transport over rough hillslope surfaces by dry ravel: Experiments and simulations with implications for nonlocal sediment flux" *Journal of Geophysical Research: Earth Surface* (2012). https://doi.org/10.1029/2011JF002229

February 24, 2012

Particle transport over rough hillslope surfaces by dry ravel: Experiments and simulations with implications for nonlocal sediment flux

Emmanuel J. Gabet, *San Jose State University*
Morgan K. Mendoza, *San Jose State University*

JOURNAL OF GEOPHYSICAL RESEARCH, VOL. 117, F01019, doi:10.1029/2011JF002229, 2012

Particle transport over rough hillslope surfaces by dry ravel: Experiments and simulations with implications for nonlocal sediment flux

Emmanuel J. Gabet[1] and Morgan K. Mendoza[1]

Received 21 September 2011; revised 22 December 2011; accepted 23 December 2011; published 24 February 2012.

[1] Past studies of hillslope evolution have typically assumed that soil creep processes are governed by a linear relationship between local hillslope angle and transport distance. The assumption of "linear diffusion" has fallen out of favor because, when coupled with an expression of mass continuity, it yields unrealistic hillslope profiles. As a consequence, a better understanding of the mechanics of sediment transport is needed. Here we report results from a series of flume experiments performed to investigate sediment transport by dry ravel, a common soil creep process in arid and semiarid environments. We find that, at gentle slopes, transport distances follow distributions characteristic of local transport. As gradients steepen, a fraction of the particles begins to exhibit nonlocal transport, and that fraction increases rapidly with slope. A stochastic discrete element model that couples an effective friction term with a shock term reproduces the results from the flume experiments, suggesting that it can be used to explore the nature of particle transport on rough surfaces. The model predicts that exponential distributions of transport distances on gentle slopes evolve into quasi-uniform distributions on steep slopes, and the transition occurs as slopes approach the angle of repose. Our results support previous findings that the angle of repose represents a threshold between friction and inertial regimes. In addition, we propose that the angle of repose represents a fuzzy boundary between local and nonlocal transport.

Citation: Gabet, E. J., and M. K. Mendoza (2012), Particle transport over rough hillslope surfaces by dry ravel: Experiments and simulations with implications for nonlocal sediment flux, *J. Geophys. Res.*, *117*, F01019, doi:10.1029/2011JF002229.

1. Introduction

[2] Regardless of climate and underlying lithology, soil-mantled hillslopes are typically convex, with flat ridges and slopes that steepen away from the divide. The ubiquity of this profile compelled *Gilbert* [1909] to propose perhaps the first hypothesis linking a sediment transport process with landscape form. Gilbert's key insight was that, on hills dominated by soil creep, the volume of sediment transported increases downslope and, thus, slopes must steepen to drive higher rates of sediment flux. Later, *Culling* [1960, 1963, 1965] provided a quantitative underpinning for Gilbert's theory by assuming that sediment flux by soil creep is linearly proportional to slope (although he expressed doubts that this assumption was strictly correct). Hillslope profiles predicted with a linear flux law, however, resemble real hillslopes only near the divide; further from the divide, predicted profiles continue to steepen whereas real hillslopes often reach an approximately constant gradient (Figure 1). *Andrews and Bucknam* [1987] were the first to address this discrepancy and developed a nonlinear equation in which flux increases asymptotically as slopes approach a threshold gradient. Similar transport equations, albeit derived via different approaches, have been proposed by others [*Gabet*, 2003; *Roering et al.*, 2001].

[3] Although hillslope profiles modeled with the nonlinear transport equation are more similar to real profiles [*Roering et al.*, 1999], they do not reproduce straight midslope sections. Indeed, models that assume that soil is a continuum and that sediment flux can be deterministically predicted as a continuous function of local hillslope gradient cannot produce linear hillslope sections. In these models, gradients must always increase downslope because temporal changes in elevation at any point on the surface are based on the divergence of the local sediment flux. Deterministic nonlinear flux laws, to an extent, help to straighten the hillslopes but, at steady state, the curvature can never be zero. This problem highlights the need for a new approach to represent hillslope sediment transport.

[4] *Tucker and Bradley* [2010] explained that continuum models, such as the one introduced by *Culling* [1960, 1963], depend on two assumptions: (1) the average sediment flux is determined by the hillslope gradient without the need to account for the exact movement of each individual soil

[1]Department of Geology, San Jose State University, San Jose, California, USA.

0148-0227/12/2011JF002229

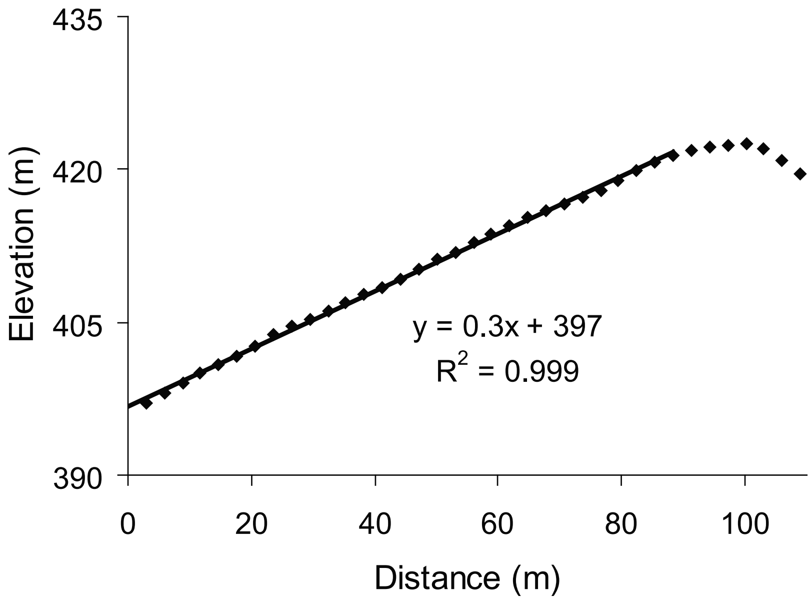

Figure 1. Hillslope profile (diamonds) near Santa Barbara, California. The midslope section is linear; field inspection of the slope showed no evidence of landslides or overland flow that could have straightened the profile. The semiarid climate and the shrubby vegetation are conducive to dry ravel. Profile extracted from 1 m digital elevation model.

particle, and (2) the gradient only needs to be known at a single point to determine the sediment flux at that point. These locality assumptions are reasonable when particles on a hillslope move only short distances relative to the length of the hillslope [*Schumer et al.*, 2009]; they are violated, however, when the distances that particles travel are large relative to hillslope length. Specifically, nonlocality occurs when the mean distance traveled by a particle tends toward infinity and, as a result, the probability distribution associated with the transport distance develops a heavy tail that is right skewed [*Tucker and Bradley*, 2010]. Whereas deep soil creep processes (e.g., shrink-swell) may be adequately represented by a continuum approach because the motion of an individual particle is impeded by its neighbors, surface creep processes (e.g., dry ravel) may exhibit nonlocal transport and, thus, may be better represented by a particle-based approach [*Furbish and Haff*, 2010; *Furbish et al.*, 2009; *Roering*, 2004].

[5] To shift from a continuum paradigm to one that is particle based, a better understanding is needed of the movement of individual particles down a rough surface and, in particular, the distribution of transport distances. Only a few studies have investigated the motion of particles in natural environments. *Schumm* [1967] tracked the movement of painted clasts on a hillslope in an arid environment. He found that the transport distance was dependent on slope but his data set is too limited to examine the distribution of distances (interestingly, Schumm dismissed some of his data because he felt that the particles had traveled too far). In a study of rain splash, *Ghahramani et al.* [2011] documented an exponential distribution of transport distances at low slopes but, at higher slopes, the distribution became heavy tailed, suggesting nonlocal transport. Given the dearth of field measurements, others have resorted to laboratory experiments to investigate particle transport. In a study of talus slope formation, *Kirkby and Statham* [1975] measured the trajectories of an irregular particle down a board roughened with gravel and found that transport distances were exponentially distributed. Similarly, *Riguidel et al.* [1994] performed experiments by rolling a ball down an inclined planar bed of closely packed homogeneous glass spheres; although this physical model simplified a more complex reality, the authors noted that it permitted a careful examination of the physics of particle motion. In their experiments, *Riguidel et al.* [1994] observed that particle behavior could be divided into three regimes. At low slopes, the particles traveled a short distance and then stopped; at intermediate slopes (5–15°), the particles reached a constant velocity; at steep slopes, the particles accelerated and began bouncing downslope. In the constant velocity regime, they found that, similar to *Kirkby and Statham* [1975], transport distances were exponentially distributed. Using a nearly identical setup as *Riguidel et al.* [1994], *Samson et al.* [1998] found that, as slopes steepen, the lateral component of travel diminishes. Abstracting particle motion even further, *Quartier et al.* [2000] rolled cylinders down a bed of homogeneous cylinders to reduce particle motion to quasi–two dimensions. They concluded that the energy of the mobile particles was dissipated by shocks from impacts with the bed and by the trapping of particles between bed roughness elements.

[6] In an important first step toward a more realistic approach to describe surface soil creep processes, *Tucker and Bradley* [2010] developed a cellular model to link the behavior of individual particles (or particle aggregates) with hillslope form. In their approach, individual particles on a slope were randomly selected and activated on the basis of their position relative to their neighbors and a probability distribution. Although the process of particle motion was represented probabilistically, the model reproduced realistic

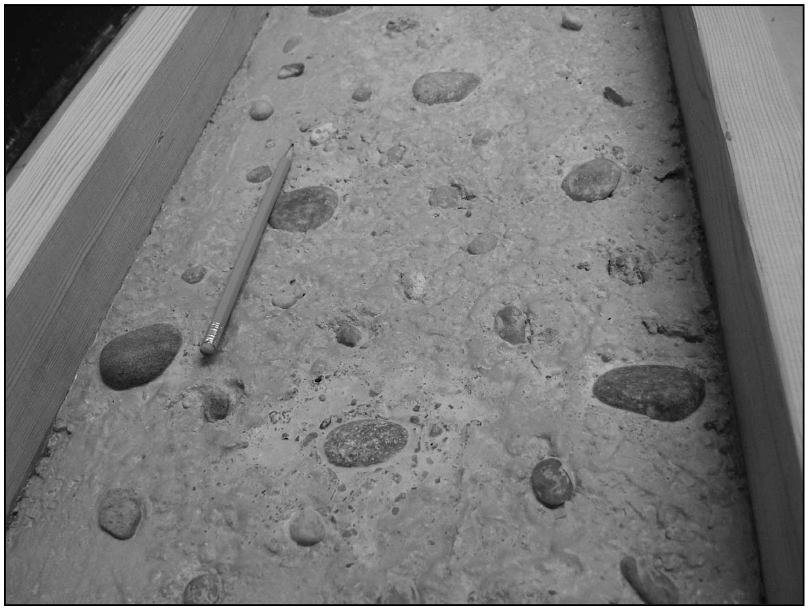

Figure 2. Photograph of flume surface. Pencil for scale.

hillslopes with convex hilltops and straight midsections. This model represents a step forward because it is discrete and nondeterministic; the probability distribution for particle motion, however, was chosen arbitrarily owing to a lack of appropriate data.

[7] Assuming an exponential probability distribution of transport distances, *Furbish and Haff* [2010] developed a theoretical approach to hillslope transport that produces slopes that are nearly linear in their midsections but the authors expressed the need for "further clarification on the physics of deposition." Taking a different path, *Foufoula-Georgiou et al.* [2010] used analytical solutions of fractional derivatives to distinguish between local transport on gentle slopes and nonlocal transport on steep slopes, an approach that also produces nearly linear profiles. Importantly, both *Furbish and Haff* [2010] and *Foufoula-Georgiou et al.* [2010] incorporate the topographic characteristics of the particles' paths.

[8] These recent papers highlight the need for: (1) measurements of the probability distribution of particle transport distances for a range of slopes, and (2) a modeling approach that incorporates the physics of particle motion. In this contribution, we investigate particle transport by dry ravel, the rolling, sliding, and bouncing of individual particles down a rough surface [*Anderson et al.*, 1959]. We chose dry ravel as the focus of our study because it is a common process in arid and semiarid environments, it can be easily studied in the laboratory, and the physics of the process can be parsimoniously described [*Gabet*, 2003; *Kirkby and Statham*, 1975; *Quartier et al.*, 2000].

2. Materials and Methods

[9] A dry ravel flume was constructed by pouring concrete into a 3 m long, 0.3 m wide wooden box and embedding 1–5 cm diameter subangular to rounded quartzite clasts (Figure 2). The numbers of clasts from each size class were chosen to yield an exponential distribution of roughness elements that could be simply parameterized in a numerical model. The specific location of each clast was random but effort was made to maintain a relatively even spacing between similarly sized rocks. With a winch, the head of the flume was raised or lowered to adjust the slope. For each experimental run, a single 1 cm diameter particle was released from a hopper at the head of the flume; the particle fell onto a ramp that propelled it down the flume, imparting it with an initial slope-parallel velocity of 0.7 m/s (sufficient to allow it to travel a short but measurable distance on gentle slopes). The transport distance was then measured and the particle removed; this was repeated 100 times at each slope setting. The angle of the flume was increased in increments of 3°, beginning at 0°. After each change of slope, the height of the hopper was adjusted to ensure that the initial velocity of the particles in the down-flume direction remained at 0.7 m/s. As the experiments progressed toward steeper slopes, some of the pebbles did not stop until reaching the end of the flume. At the flume angle of 30°, all 100 pebbles rolled to the end and the experiment was terminated.

[10] The roughness of the flume was characterized by measuring its elevation along width-parallel transects at 1 cm intervals. Transects were taken along the length of the flume at 10 cm intervals, for a total of 28 width-parallel transects. The relief along each transect was calculated by subtracting the mode of the transect elevations from each measurement and taking the absolute value of the result. The flume relief measurements were divided by the diameter of the experimental particle (1 cm) to render them dimensionless. A histogram of these relative roughness values reveals an exponential distribution with a mean of 0.17 (Figure 3).

3. Results

[11] Each particle followed a unique path as it encountered a random sequence of roughness elements. The journey

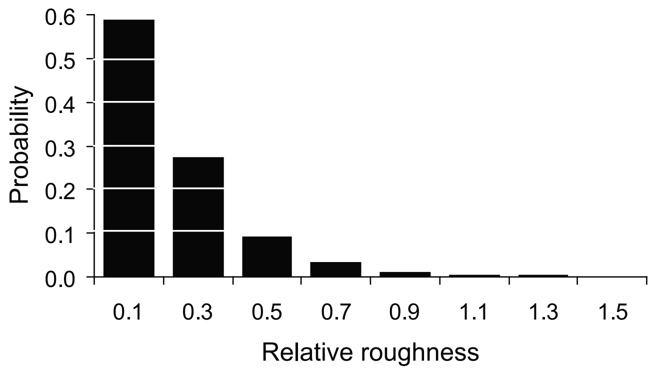

Figure 3. Distribution of relative roughness values for the flume surface (n = 812).

of most particles could be placed into three broad categories: (1) some particles rolled off the ramp, immediately encountered an embedded clast and stopped; (2) some particles came down the ramp, slowed down after hitting a medium-size clast, rolled around it, accelerated a bit, slowed down after hitting another medium-size clast, and continued to trickle down the flume until eventually rolling to a stop; and (3) other particles rolled off the ramp into a relatively smooth area, accelerated, hopped over or rolled around a few medium-size roughness elements, and then rolled into a large clast or the flume bottom and stopped. At all slope settings (except the steepest, 30°), all path types were represented although type 1 paths dominated at lower slopes and type 3 paths dominated at steeper slopes. Because these three types of motion are similar to what others have observed under more idealized conditions [*Quartier et al.*, 2000; *Riguidel et al.*, 1994; *Samson et al.*, 1998], the trajectories of the particles in our flume appear to belong to a general class of behaviors characteristic of particles on rough surfaces and are not unique to our particular experimental setup.

[12] The average distance traveled by the pebbles increased nonlinearly with the flume angle up to 15° (Figure 4a). At 3°, there is an anomalous dip in the average transport distance; however, it is not statistically lower than the average transport distance at 0° (p value = 0.15). Particles began reaching the end of the flume at 18° and the proportion of pebbles rolling to the end of the flume increased rapidly as slopes steepened (Figure 4b). For these steeper slopes, an average travel distance was calculated only from the particles that did not reach the end of the flume; these averages are not meant to represent an aggregate mean transport distance but are used to compare with model results.

[13] At low slopes, the distribution of travel distances is tightly clustered around low values (Figure 5a); as slopes steepen, the distribution becomes humped and its right tail stretches out (Figure 5b). When the flume reaches angles where a significant proportion of the particles rolled to the end, 18–24°, the distribution flattens and becomes quasi-uniform (Figure 5c). At 27°, only 4 particles stopped before the flume end, making it difficult to draw conclusions about the shape of the distribution. In general, as slopes become steeper, the shape of the distribution evolves to accommodate a greater range of possible transport distances; this conclusion is well captured by the increase in variance (Figure 4a).

4. Numerical Model

4.1. Governing Equations

[14] A discrete element model was developed to assess whether the transport of a particle down the flume could be simulated numerically. In the model, a particle was given an initial velocity, v, and the distance traveled, x, was determined according to:

$$x = v\Delta t \tag{1}$$

where Δt is the time step. A time step of 0.1 s was deemed appropriate because it represents a travel distance of $\sim$1–10 cm, similar to the distances between major roughness elements. We note that the model results are sensitive to the time step; for example, in simulations with time steps of order 1 s, particles would sometimes reach the end of the model space too soon because of limited interaction with the surface.

[15] The velocity was updated at each time step with:

$$v = v + a\Delta t. \tag{2}$$

Quartier et al. [2000] concluded that the acceleration of a particle on a rough bed can be represented with a Coulomb-like friction term and a velocity-dependent shock term such that

$$a = g(\sin\theta - \mu\cos\theta) - \kappa v^w \tag{3}$$

where g is gravitational acceleration, θ is slope angle, μ is a dynamic friction coefficient, κ is a shock coefficient, and w is a constant. At each time step, a value for μ was randomly chosen from a probability distribution to simulate the random trajectory of a particle down the rough surface (see section 4.2.). In previous granular flow experiments, some have found a value of 1 for the exponent w [*Samson et al.*, 1998] while others found a value of 2 [*Quartier et al.*, 2000]; here, a set of simulations was done with each value to compare results. When w = 1 (i.e., linear shock), κ has units of s^{-1}; when w = 2 (i.e., quadratic shock), it has units of m^{-1}.

[16] The particle was advanced, according to equations (1)–(3), until its velocity became nonpositive or it reached the end of the model space. Because the value of κ was unconstrained, its value was systematically varied until it produced the best match to the flume data. For each value of κ, t tests (α = 0.05) were performed to compare the modeled average transport distance to the flume data, and the best κ values were determined on the basis of how many average transport distances the model correctly simulated. The comparisons were made for the slopes in the range of 0–24°. At 27°, the average transport distance on the flume was calculated from only 4 particles because the other 96 reached the end of the flume and, thus, comparisons with the model results at this slope are tenuous; no particles remained on the flume at 30°.

4.2. Probability Distribution of μ

[17] The results from the flume experiments at 0° slope were used to construct a distribution of μ values. *Kirkby and Statham* [1975] and *Gabet* [2003] demonstrated that

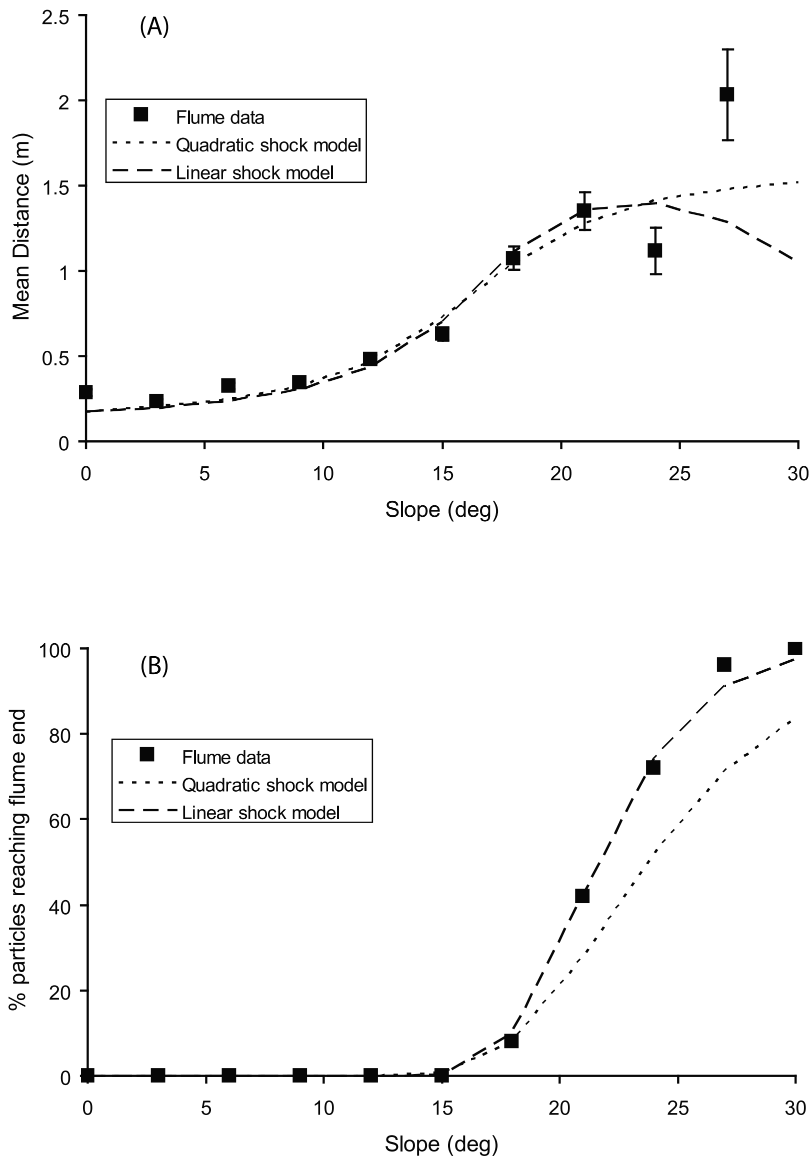

Figure 4. (a) Mean transport distances: model versus flume data. Error bars equal 1 SE. Both models performed equally well; comparing the results for the steeper slopes is tenuous because only a small number of particles remained on the flume. (b) Proportion of particles reaching the end of the flume: model versus flume data. The linear shock model performed better than the quadratic model.

particles imparted with an initial velocity (v_0) will travel a distance, d, according to:

$$d = \frac{v_0^2}{2g(\mu\cos\theta - \sin\theta)}. \quad (4)$$

Equation (4) assumes that the Coulomb friction term in equation (3), which represents the trapping of particles [*Quartier et al.*, 2000], is primarily responsible for the dissipation of energy. We propose that, when the flume was inclined at 0° and particle velocities were at their lowest, energy losses from velocity-dependent shock were small relative to losses from friction. Rearranging equation (4) yields

$$\mu = \frac{v_0^2}{2gd\cos\theta} + \tan\theta \quad (5)$$

so that the coefficient of friction can be estimated from each measured transport distance. In addition to minimizing the effect of shocks, the results from the experiments at 0° were used because (1) the travel distances were short and, therefore, the calculated μ spatially averages over only a small interval, and (2) the pebbles bounced the least and, thus, spent the most time in contact with the flume surface.

[18] The μ values estimated with this approach follow an exponential distribution with a mean of 0.25 (Figure 6). It is important to emphasize that these μ values reflect the shape of the moving particles and not just the topography of the flume surface. Nevertheless, the similarities between the distributions of the friction coefficient and the relative roughness measured directly from the flume surface (Figure 3) suggest a direct mechanistic link between the two [*Kirkby and Statham*, 1975]. Finally, we note that, although

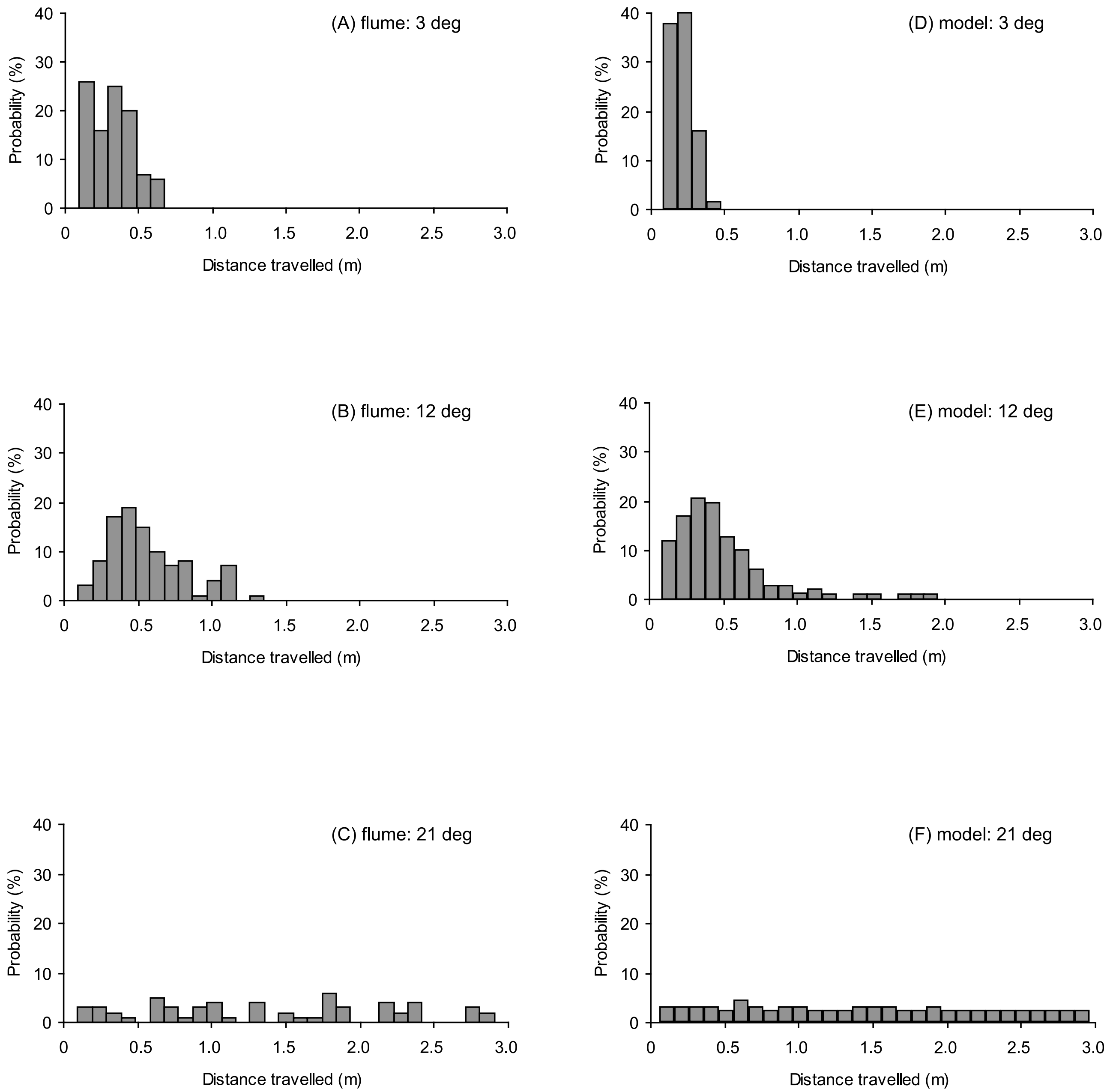

Figure 5. Comparison of (a–c) measured and (d–f) modeled transport distance distributions for three selected slope angles. Only the results from the linear shock model are shown because of its overall better performance. The modeled distributions are fuller because of the greater number of particles.

we performed our experiments with a single particle size and only one initial velocity, *Kirkby and Statham* [1975] and *Statham* [1976] demonstrated that equation (4) applies to a range of particle sizes and initial velocities.

4.3. Simulations of Flume Experiments

[19] To simulate the flume experiments, 10^6 particles began with an initial velocity of 0.7 m/s at the top of a 3 m long model space. The quadratic shock model ($\kappa = 0.0262$) and the linear shock model ($\kappa = 0.0175$) performed equally well in simulating the average transport distances observed in the flume experiments (Figure 4a). With the quadratic shock model, there was no statistically significant difference (t test, $\alpha = 0.05$) between the means of the experimental and modeled transport distances for $\theta = 3$, 9, 12, 18, and 21°. With the linear shock model, there was no statistically significant difference ($\alpha = 0.05$) between the means of the transport distances for $\theta = 9$, 12, 18, 21, and 24°. Both models, therefore, correctly simulated the average transport distance for 5 out of 9 slope angles. Note that we are applying a fairly strict standard for assessing the performance of our model; similar studies [e.g., *Batrouni et al.*, 1996] have relied on a visual comparison of the fit between model and experimental results.

[20] Although both models performed equally well in simulating average transport distance, they differentiated themselves

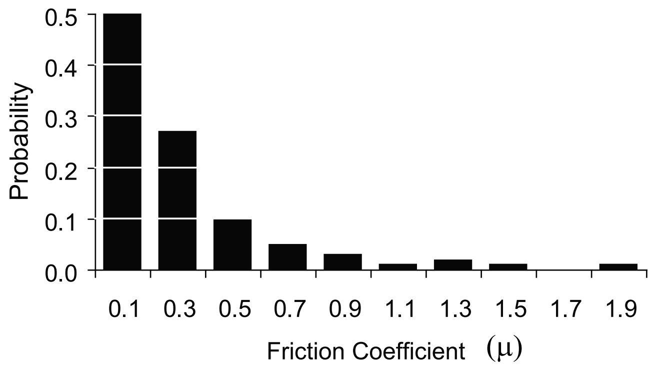

Figure 6. Probability distribution of the coefficient of dynamic friction calculated from particle transport distance.

in their prediction of the proportion of particles reaching the end of the flume (Figure 4b). The quadratic shock model was incorrect at the three steepest slopes (Fisher's exact test, α = 0.05), a critical mismatch with the flume data. In contrast, the linear shock model correctly predicted the proportion of particles reaching the bottom of the flume at every slope (Fisher's exact test, α = 0.05).

[21] Finally, the model reproduced reasonably well the probability distribution of transport distances (Figures 5d–5f). As with the average transport distances, however, the model performed better at steeper slopes than gentler slopes. For example, the model generally underpredicted the average distances for slopes < 9° (Figure 4a) and the modeled distances at 3° form a slightly tighter distribution than the measured distances. This bias is most likely a consequence of the assumption that the shock term was negligible in our calculations of μ from the experimental data at 0° (equation (5)). In contrast, the numerical model accounts for shocks and, thus, incorporates an extra component of energy dissipation. Note that, for most combinations of velocity, μ, and θ, the shock term contributes only a small percentage (order 1%) to the overall deceleration; for certain ranges of values of these parameters, however, the shock term accounts for a more significant percentage (order 10%). The shock term is particularly effective at slowing down rapidly moving particles at intermediate slopes.

4.4. Modeling Particle Transport at the Hillslope Scale

[22] Given the better overall performance of the linear shock model, it was used to investigate particle trajectories at the hillslope scale. As in the flume simulations, μ values were randomly chosen from the exponential distribution (Figure 6) and κ was set to 0.0175. Although the flume surface is likely harder and smoother than most real hillslopes where dry ravel is active, the results should allow some general conclusions on the nature of hillslope transport. Initial velocities were randomly selected from an exponential distribution with a mean of 0.5 m/s; we emphasize that the characteristics of this distribution are not based on any data but are, simply, reasoned guesses. Under natural conditions, a particle's initial velocity could come from a variety of sources, such as a fall from a cliff face [*Statham*, 1976], animal disturbance [*Anderson et al.*, 1959], or the destruction of vegetation dams during a fire [*Lamb et al.*, 2011]. Finally, the model space was extended to simulate a linear, 100 m long hillslope.

[23] At slopes up to 21°, the model predicts an exponential distribution of transport distances (Figures 7 and 8a). As slopes steepen, the right tail of the distribution thickens and the distribution becomes quasi-uniform (Figures 8b–8d). At even the steepest slopes, a fraction of the particles immediately stopped because their initial velocities were too low to overcome the initial resistance and develop sufficient kinetic energy to continue down the slope. Admittedly, while the general evolution of the transport distributions is likely realistic, the roughness parameters derived from the flume experiments produce actual distributions that may be unrealistic for most natural slopes where dry ravel is an important process. For example, the model predicts that ∼50% of the particles activated on a 30° slope would travel more than 100 m (Figure 8b) whereas this result might be expected at steeper inclines on natural hillslopes. Finally, note that, at low slopes, the transport distributions of the flume experiments and simulations were humped whereas the distributions from

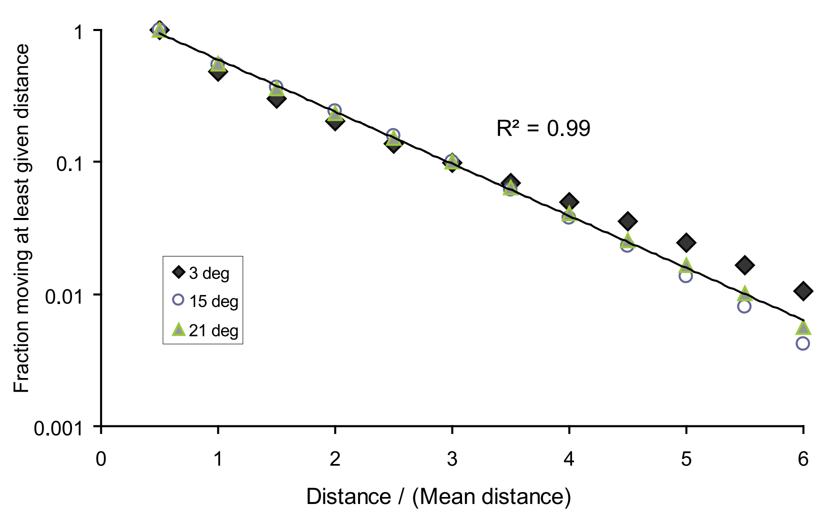

Figure 7. Cumulative distributions of normalized modeled transport distances. In the range of 3–21°, distributions are strongly exponential. Note the semilogarithmic axes.

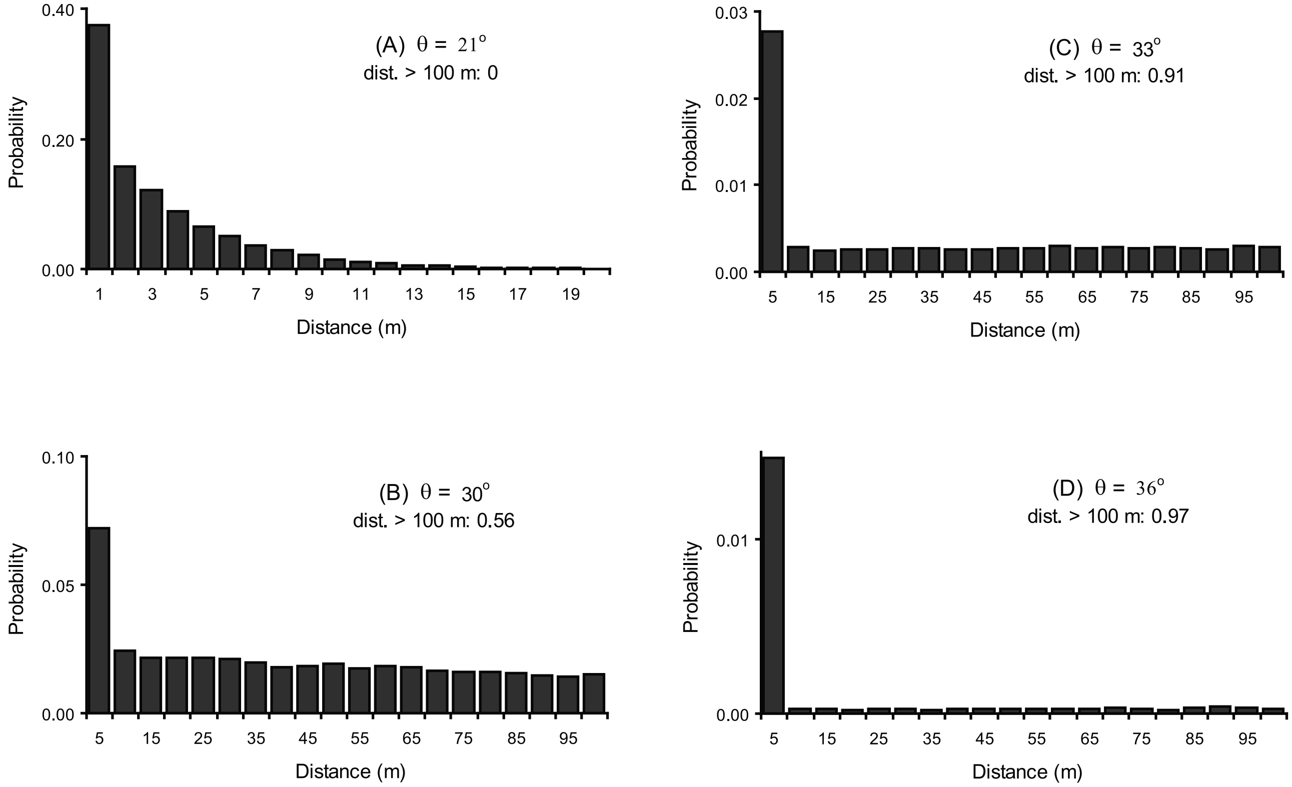

Figure 8. Probability distributions of transport distance as a function of slope. The fraction of particles reaching the end of the model space is noted as "dist. > 100 m: #." For clarity, particles that traveled <0.01 m were filtered from the results. Note the different scales on the x axes.

these simulations are exponential. The variation arises from the difference in initial velocities; in the flume simulations, v_0 was held constant whereas, in the hillslope simulations, v_0 followed an exponential distribution.

5. Discussion

5.1. Simulating Dry Ravel

[24] Given the complex three-dimensional motion of an irregular particle over a rough heterogeneous bed, a set of physical equations that would fully describe its trajectory would be unwieldy and impractical for exploring sediment transport down hillslopes. The goal, therefore, should be to describe the motion phenomonologically in the most parsimonious fashion possible [*Forterre and Pouliquen*, 2008]. In a strict sense, the Coulomb-friction term in equation (3) is only appropriate for the classic "sliding block on a plane" scenario; nevertheless, it is commonly applied in the modeling of granular flows [*Iverson and Denlinger*, 2001; *Pouliquen and Forterre*, 2002]. As argued by *Quartier et al.* [2000] and as suggested by our results (Figure 4), equation (3) simulates reasonably well the macroscopic behavior of a single particle while incorporating only one unconstrained constant, κ. In addition, although *Quartier et al.* [2000] derived equation (3) on the basis of the two-dimensional trajectories of discs down a homogeneous surface, our results suggest that the random sequencing of the friction coefficient allows their approach to be expanded to the more complicated three-dimensional motions of irregular particles down a rough, heterogeneous bed. We note that, after testing our approach, we tested a "bouncing" model on the basis of the standard equations of motion [e.g., *Batrouni et al.*, 1996], with momentum loss occurring via a coefficient of restitution. Despite extensive searches through parameter space, this model did not perform as well as ours.

[25] Because our model accounts for the kinetic energy of particles, particles in motion retain a memory of their journey. Particles exhibiting nonlocal transport may pass through "neighborhoods" that have different slopes and surface roughness. The position and velocity at any point in time of a particle in motion thus integrates the properties of the neighborhoods through which it has passed. In other words, a moving particle's state retains information about where it has been: given the same initial conditions, a particle that has recently passed through a rough patch will be traveling slower than one crossing a smooth patch. The slower-moving particle is, thus, more likely to arrest its motion than its faster counterpart. In the cellular model developed by *Tucker and Bradley* [2010], the particles have no memory as they move downslope although the authors emphasize that their model could be modified to keep track of particle momentum.

[26] The stochastic nature of sediment transport revealed by the flume experiments and the model brings to light some of the limitations of the deterministic, continuum approach. The deterministic nonlinear flux equation proposed by *Gabet* [2003] for dry ravel is similar in form to those derived by others to describe more general soil creep processes [*Andrews and Bucknam*, 1987; *Roering et al.*, 1999]. The distinguishing feature of these equations is an asymptotic

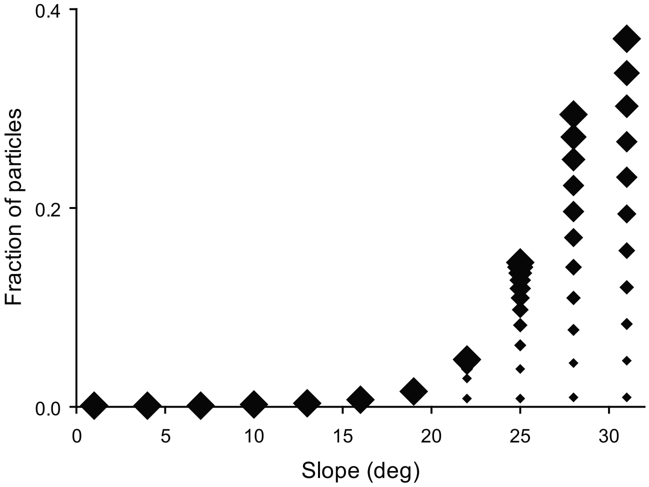

Figure 9. Modeled sediment flux versus slope. Symbol size is proportional to downslope position where the flux was measured: the smallest symbol indicates the numbers of particles crossing a contour line 1 m from the divide; the largest symbol indicates the number of particles crossing a contour line 41 m downslope of the divide; and the distance between each intermediate position is 4 m. At slopes <20, flux is relatively independent of position, and thus the symbols overlap each other. At steeper slopes, downslope positions "see" more particles because of the longer contributing area and the greater transport distances.

increase in flux as hillslopes approach a threshold gradient; beyond the threshold gradient, sediment flux becomes infinitely high. However, as shown in our results, the threshold is fuzzy rather than distinct. Indeed, at slopes as low as 18°, some proportion of the particles traveled across the entire domain (Figure 4b). Our particle-based approach, as well as *Tucker and Bradley*'s [2010], simulate well the fuzzy, stochastic nature of the threshold: in both cases, the number of particles reaching the lower boundary increases with slope. The ability to model correctly the potential for long-range travel is important for understanding the evolution of linear slopes. Particles that travel to the bottom of the slope essentially disappear from the hillslope and, thus, gradients do not have to increase downslope in order to accommodate their passage [cf. *Gilbert*, 1909]. In addition, our results suggest that, even at very steep slopes, some proportion of activated particles do not travel very far at all. Thus, for a range of slopes steeper than the threshold gradient, the gross sediment flux never becomes infinite.

5.2. Local Versus Nonlocal Transport and the Angle of Repose

[27] The hillslope-scale model results suggest that an exponential distribution of transport distances evolves into a long-tailed distribution as slopes increase. Exponential distributions are characteristic of local transport [*Foufoula-Georgiou et al.*, 2010; *Ganti et al.*, 2010]. In the case of dry ravel on gentle slopes, the kinetic energy of particles is low and their motion can be stopped by a wide range of roughness elements. Thus, for each increment of travel, there is an equal probability that the particle will become trapped; this is a classic Poisson process that yields exponential distributions [*Kirkby and Statham*, 1975; *Riguidel et al.*, 1994]. At this range of slopes, dry ravel motion could be considered to be dominated by frictional, rather than inertial, forces [*Riguidel et al.*, 1994].

[28] On steeper slopes, particles are more likely to accelerate and, thus, their kinetic energy increases such that only the largest roughness elements are able to arrest their motion. Dry ravel motion at these steeper slopes, therefore, could be considered to be dominated by inertial forces [*Riguidel et al.*, 1994]. Because particles can accelerate on these slopes, the probability that a particle may become trapped decreases with distance, leading to the long-tailed quasi-uniform distribution of transport distances. As demonstrated by others [*Foufoula-Georgiou et al.*, 2010; *Ganti et al.*, 2010], long-tailed distributions are a hallmark of nonlocal transport.

[29] The term "angle of repose" takes on various meanings, depending on context [*Statham*, 1976]; we use it here in the sense of the angle of a pile of particles formed through the accumulation of sediment dropping from above (i.e., the angle of residual shear). Values for the angle of repose commonly spans values from 25 to 35° [*Selby*, 1993], a range that matches the transition from exponential to uniform transport distributions (Figure 8). This threshold angle emerges spontaneously in our model even though the average value of μ used in the exponential distribution, 0.25, corresponds to 14° (note: tan 30° corresponds to the 90th percentile of the μ distribution). The angle of repose, therefore, appears to mark the transition between frictional and inertial regimes [*Riguidel et al.*, 1994] and between local and nonlocal transport. For instance, *Govers and Poesen* [1998] documented the motion of particles on a scree slope (presumably near the angle of repose) and found that the distribution of transport distances had a heavier tail than predicted according to an exponential distribution.

5.3. Sediment Flux As a Function of Slope and Distance

[30] Because the travel distance by raveling particles can be relatively long, especially on steeper slopes, the sediment flux at any particular spot on a hillslope may be dependent on its distance from the divide. To assess the relative importance of slope and downslope distance on sediment flux, a series of model runs was performed in which 10^6 particles were released at random positions on a linear 50 m hillslope and the number of particles passing a particular point was recorded. The initial velocities and μ values were parameterized as in the previous hillslope simulations. In the range of angles 0–19°, transport distances are short and the sediment flux can be described solely as a function of slope (Figure 9). With increasing slope, however, travel distances lengthen and positions further downslope are "seeing" particles that began their journey outside of the local neighborhood. In other words, at steeper slopes, the length of the contributing area becomes increasingly important. Similarly, *Foufoula-Georgiou et al.* [2010] concluded that hillslope transport is local on gentle slopes but nonlocal on steeper slopes. These results suggest that the nonlinear increase in dry ravel sediment flux with slope recorded by sediment traps in the work of *Gabet* [2003] may have been primarily due to an increase in transport distance, rather than sediment volume. Because the sediment traps were installed on a convex hillslope, the apparent increase in flux with gradient may,

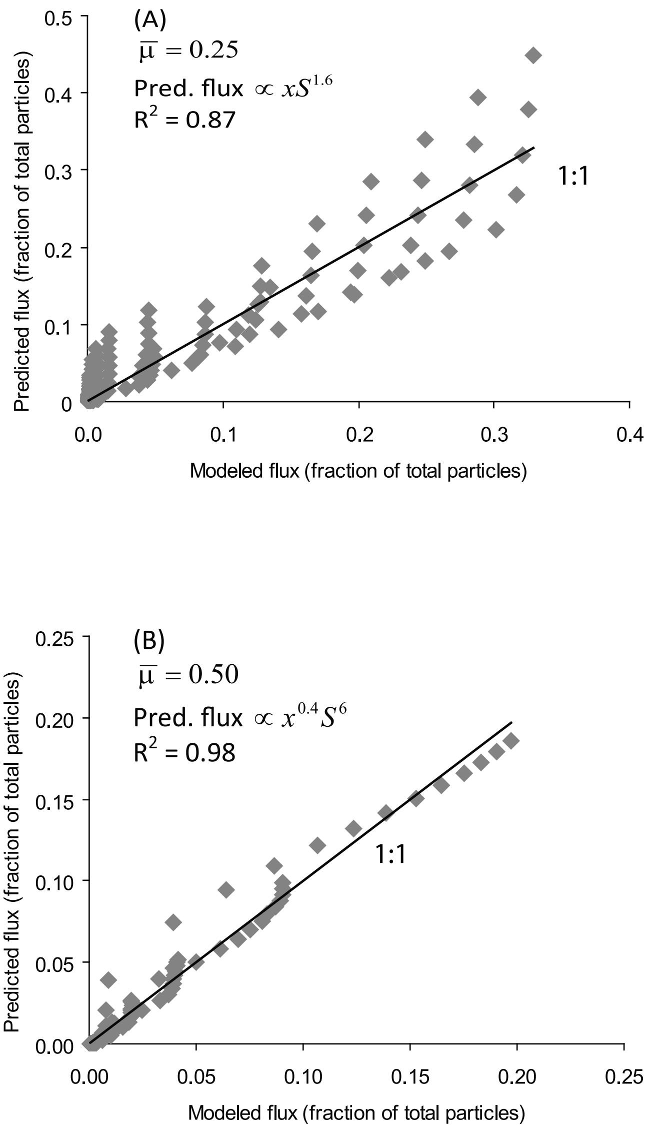

Figure 10. Sediment flux as a function of slope and distance from the divide. (a) With a relatively low coefficient of friction, sediment flux is strongly dependent on contributing length (x). (b) Doubling the friction coefficient damps particle travel and decreases the influence of contributing length while increasing the importance of slope.

instead, have been an increase in flux with downslope distance. *Tucker and Bradley* [2010] offered a similar critique of efforts to parameterize the nonlinear soil creep equation.

[31] Although we do not advocate the use of deterministic models to describe sediment flux by soil creep processes on steep slopes, they are useful for gauging the importance of various parameters. For example, *Carson and Kirkby* [1972] proposed a general sediment flux equation that incorporates local slope and the length of contributing hillslope:

$$q_s \propto x^m S^n \tag{6}$$

where q_s is sediment flux (L^2/T), x is distance from the upper boundary, S is slope, and m and n are fitted parameters. Whereas flux equations for soil creep processes have typically assumed that $m = 0$, our flume and model results suggest that, at least for dry ravel, $m > 0$. To explore the relative importance of contributing area, slope, and surface properties on dry ravel flux, two sets of model runs were performed for the range of slopes 1–49°. In one set of model runs, the mean value of μ ($\bar{\mu}$) was set to 0.25, and in the other, $\bar{\mu}$ was doubled to 0.50. Fitting equation (6) to the model results where $\bar{\mu} = 0.25$ yields $m = 1.0$ and $n = 1.6$ (Figure 10a), thus suggesting an important dependency on contributing area. Doubling the average friction coefficient, the slope exponent increases to 6 but the exponent on the downslope distance drops to 0.4 (Figure 10b). Transport, therefore, becomes increasingly slope-dependent and local as the surface dissipates more energy. Surfaces that allow particles to retain more of their energy, in contrast, promote nonlocal transport.

5.4. Evolution of Talus Piles

[32] A thought experiment reveals how the evolution of transport distributions with increasing gradient could be used to explain the growth of talus piles formed from the accumulation of weathered material falling from a cliff face [*Statham*, 1976]. Initially, clasts collect at the base of the cliff forming a low pile with gentle slopes. The low slopes lead to an exponential distribution of transport distances of rocks falling on the pile from above; during this stage, the upper portion of the pile accumulates material faster than the lower portion, and the pile steepens as it grows allometrically. Eventually, as the slope approaches the angle of repose, rocks falling on the top of the pile follow a more uniform distribution of travel distances; at this stage, the pile experiences isometric growth.

6. Conclusion

[33] Although it has been useful to assume that the flux from soil creep processes is linearly related to slope, recent efforts have attempted to represent particle transport more realistically. These efforts have led to the recognition that (1) particle path lengths are not deterministic, and (2) particles may travel significant distances relative to hillslope extent. To examine the dynamics of particle transport, we performed experiments and model simulations that explore the process of dry ravel in arid and semiarid environments. The governing equation for the numerical model couples a Coulomb-like friction term and a linear shock term that accounts for energy dissipation via impacts. Our results reveal how the distribution of transport distance varies as a function of slope for dry ravel. On relatively gentle slopes, transport distances are well represented by exponential distributions but, as slopes steepen, the distributions become more uniform. This transition begins as slopes approach the angle of repose, suggesting that it represents a threshold, albeit fuzzy, between local and nonlocal sediment transport. In addition, our results suggest that sediment flux by dry ravel is not purely slope dependent and that the upslope contributing area may be an important factor.

[34] **Acknowledgments.** We are grateful to the GEOMORPHLIST community for their helpful suggestions. Discussions with D. Furbish, J. Roering, and M. Lamb were invaluable. We thank G. Tucker and the anonymous reviewers for their incisive comments and generous suggestions; we are especially grateful to the reviewer who shared with us his/her “bouncing particle” code.

References

Anderson, H. W., G. B. Coleman, and P. J. Zinke (1959), Summer slides and winter scour, dry-wet erosion in Southern California mountains, *Tech. Pap. PSW-36*, Pac. Southwest For. and Range Exp. Stn., U.S. Dep. of Agric. For. Serv., Washington, D. C.

Andrews, D. J., and R. C. Bucknam (1987), Fitting degradation of shoreline scarps by a nonlinear diffusion model, *J. Geophys. Res.*, *92*, 12,857–12,867, doi:10.1029/JB092iB12p12857.

Batrouni, G. G., S. Dippel, and L. Samson (1996), Stochastic model for the motion of a particle on an inclined rough plane and the onset of viscous friction, *Phys. Rev. E*, *53*, 6496–6503, doi:10.1103/PhysRevE.53.6496.

Carson, M. A., and M. J. Kirkby (1972), *Hillslope Form and Process*, 475 pp., Cambridge Univ. Press, New York.

Culling, W. E. H. (1960), Analytical theory of erosion, *J. Geol.*, *68*, 336–344, doi:10.1086/626663.

Culling, W. E. H. (1963), Soil creep and the development of hillside slopes, *J. Geol.*, *71*, 127–161, doi:10.1086/626891.

Culling, W. E. H. (1965), Theory of erosion on soil-covered slopes, *J. Geol.*, *73*, 230–245.

Forterre, Y., and O. Pouliquen (2008), Flows of dense granular media, *Annu. Rev. Fluid Mech.*, *40*, 1–24, doi:10.1146/annurev.fluid.40.111406.102142.

Foufoula-Georgiou, E., V. Ganti, and W. E. Dietrich (2010), A nonlocal theory of sediment transport on hillslopes, *J. Geophys. Res.*, *115*, F00A16, doi:10.1029/2009JF001280.

Furbish, D. J., and P. K. Haff (2010), From divots to swales: Hillslope sediment transport across divers length scales, *J. Geophys. Res.*, *115*, F03001, doi:10.1029/2009JF001576.

Furbish, D. J., P. K. Haff, W. E. Dietrich, and A. M. Heimsath (2009), Statistical description of slope-dependent soil transport and the diffusion-like coefficient, *J. Geophys. Res.*, *114*, F00A05, doi:10.1029/2009JF001267.

Gabet, E. J. (2003), Sediment transport by dry ravel, *J. Geophys. Res.*, *108*(B1), 2049, doi:10.1029/2001JB001686.

Ganti, V., M. M. Meerschaert, E. Foufoula-Georgiou, E. Viparelli, and G. Parker (2010), Normal and anomalous diffusion of gravel tracer particles in rivers, *J. Geophys. Res.*, *115*, F00A12, doi:10.1029/2008JF001222.

Ghahramani, A., I. Yoshiharu, and S. M. Mudd (2011), Field experiments constraining the probability distribution of particle travel distances during natural rainstorms on different slope gradients, *Earth Surf. Processes Landforms*, doi:10.1002/esp.2253, in press.

Gilbert, G. K. (1909), The convexity of hillslopes, *J. Geol.*, *17*, 344–350, doi:10.1086/621620.

Govers, G., and J. Poesen (1998), Field experiments on the transport of rock fragments by animal trampling on scree slopes, *Geomorphology*, *23*, 193–203, doi:10.1016/S0169-555X(98)00003-8.

Iverson, R. M., and R. P. Denlinger (2001), Flow of variably fluidized granular masses across three-dimensional terrain: 1. Coulomb mixture theory, *J. Geophys. Res.*, *106*, 537–552, doi:10.1029/2000JB900329.

Kirkby, M. J., and I. Statham (1975), Surface stone movement and scree formation, *J. Geol.*, *83*, 349–362, doi:10.1086/628097.

Lamb, M. P., J. S. Scheingross, W. H. Amidon, E. Swanson, and A. Limaye (2011), A model for fire-induced sediment yield by dry ravel in steep landscapes, *J. Geophys. Res.*, *116*, F03006, doi:10.1029/2010JF001878.

Pouliquen, O., and Y. Forterre (2002), Friction law for dense granular flows: Application to the motion of a mass down a rough inclined plane, *J. Fluid Mech.*, *453*, 133–151, doi:10.1017/S0022112001006796.

Quartier, L., B. Andreotti, S. Douady, and A. Daerr (2000), Dynamics of a grain on a sandpile model, *Phys. Rev. E*, *62*, 8299–8307, doi:10.1103/PhysRevE.62.8299.

Riguidel, F., R. Jullien, G. H. Ristow, A. Hansen, and D. Bideau (1994), Behaviour of a sphere on a rough surface, *J. Phys. I*, *4*, 261–272, doi:10.1051/jp1:1994106.

Roering, J. J. (2004), Soil creep and convex-upward velocity profiles: Theoretical and experimental investigations of disturbance-driven sediment transport on hillslopes, *Earth Surf. Processes Landforms*, *29*, 1597–1612, doi:10.1002/esp.1112.

Roering, J. J., J. W. Kirchner, and W. E. Dietrich (1999), Evidence for nonlinear, diffusive sediment transport on hillslopes and implications for landscape morphology, *Water Resour. Res.*, *35*, 853–870, doi:10.1029/1998WR900090.

Roering, J. J., J. W. Kirchner, and W. E. Dietrich (2001), Hillslope evolution by nonlinear, slope-dependent transport: Steady state morphology and equilibrium adjustment timescales, *J. Geophys. Res.*, *106*, 16,499–16,513, doi:10.1029/2001JB000323.

Samson, L., I. Ippolito, G. G. Batrouni, and J. Lemaitre (1998), Diffusive properties of motion on a bumpy plane, *Eur. Phys. J. B*, *3*, 377–385, doi:10.1007/s100510050325.

Schumer, R., M. M. Meerschaert, and B. Baeumer (2009), Fractional advection-dispersion equations for modeling transport at the Earth surface, *J. Geophys. Res.*, *114*, F00A07, doi:10.1029/2008JF001246.

Schumm, S. A. (1967), Rates of surficial rock creep on hillslopes in western Colorado, *Science*, *155*, 560–562, doi:10.1126/science.155.3762.560.

Selby, M. J. (1993), *Hillslope Materials and Processes*, 451 pp., Oxford Univ. Press, Oxford, U. K.

Statham, I. (1976), A scree slope rockfall model, *Earth Surf. Processes*, *1*, 43–62, doi:10.1002/esp.3290010106.

Tucker, G. E., and D. N. Bradley (2010), Trouble with diffusion: Reassessing hillslope erosion laws with a particle-based model, *J. Geophys. Res.*, *115*, F00A10, doi:10.1029/2009JF001264.

E. J. Gabet and M. K. Mendoza, Department of Geology, San Jose State University, San Jose, CA 95192, USA. (manny.gabet@sjsu.edu)